PAIN

$Na_V1.7$ target modulation and efficacy can be measured in nonhuman primate assays

Richard L. Kraus[1]*, Fuqiang Zhao[1], Parul S. Pall[1], Dan Zhou[1], Joshua D. Vardigan[1], Andrew Danziger[1], Yuxing Li[1], Christopher Daley[1], Jeanine E. Ballard[1], Michelle K. Clements[1], Rebecca M. Klein[1], Marie A. Holahan[1], Thomas J. Greshock[1], Ronald M. Kim[1], Mark E. Layton[1], Christopher S. Burgey[1], Jordi Serra[2], Darrell A. Henze[1], Andrea K. Houghton[1]

Humans with loss-of-function mutations in the $Na_V1.7$ channel gene (SCN9A) show profound insensitivity to pain, whereas those with gain-of-function mutations can have inherited pain syndromes. Therefore, inhibition of the $Na_V1.7$ channel with a small molecule has been considered a promising approach for the treatment of various human pain conditions. To date, clinical studies conducted using selective $Na_V1.7$ inhibitors have not provided analgesic efficacy sufficient to warrant further investment. Clinical studies to date used multiples of in vitro IC_{50} values derived from electrophysiological studies to calculate anticipated human doses. To increase the chance of clinical success, we developed rhesus macaque models of action potential propagation, nociception, and olfaction, to measure $Na_V1.7$ target modulation in vivo. The potent and selective $Na_V1.7$ inhibitors SSCI-1 and SSCI-2 dose-dependently blocked C-fiber nociceptor conduction in microneurography studies and inhibited withdrawal responses to noxious heat in rhesus monkeys. Pharmacological $Na_V1.7$ inhibition also reduced odor-induced activation of the olfactory bulb (OB), measured by functional magnetic resonance imaging (fMRI) studies consistent with the anosmia reported in $Na_V1.7$ loss-of-function patients. These data demonstrate that it is possible to measure $Na_V1.7$ target modulation in rhesus macaques and determine the plasma concentration required to produce a predetermined level of inhibition. The calculated plasma concentration for preclinical efficacy could be used to guide human efficacious exposure estimates. Given the translatable nature of the assays used, it is anticipated that they can be also used in phase 1 clinical studies to measure target modulation and aid in the interpretation of phase 1 clinical data.

INTRODUCTION

The genomics of pain continue to be unraveled (*1*–*6*), providing genetic support for a number of approaches to developing analgesics. Genetic links between peripheral voltage-gated sodium (Na_V) channels and enhanced or diminished pain response in humans have been found (*7*–*9*), and potential avenues to precision pain medicines targeting ion channels have been identified (*10*). In addition to genetic evidence, drugs with nonselective sodium channel–blocking activities, such as anesthetics, anticonvulsants, and antidepressants, are used in current pain management paradigms (*11*–*16*). Unfortunately, the effectiveness of nonselective sodium channel blockers is often limited by central nervous system (CNS) and cardiovascular side effects (*15*). However, selective inhibition of sodium channels specifically involved in pain pathways has the potential to improve efficacy and safety (*8*, *10*, *17*). To date, nine related Na_V channels have been identified, namely, $Na_V1.1$, $Na_V1.2$, $Na_V1.3$, $Na_V1.4$, $Na_V1.5$, $Na_V1.6$, $Na_V1.7$, $Na_V1.8$, and $Na_V1.9$ (*18*). $Na_V1.7$, $Na_V1.8$, and $Na_V1.9$ channels are predominantly expressed in primary nociceptive afferents and have been linked to human monogenic pain disorders.

The $Na_V1.7$ channel has received heightened attention from the pain research field (*19*) as loss-of-function mutations in the gene SCN9A encoding $Na_V1.7$ have been associated with congenital insensitivity to pain (*20*). In contrast, gain-of-function mutations in SCN9A lead to $Na_V1.7$ mediated neuronal hyperexcitability and have been identified as the underlying mechanism of hereditary pain disorders such as erythromelalgia, paroxysmal extreme pain disorder, and some small fiber neuropathies (*21*, *22*). Consequently, there has been considerable research interest aimed at developing selective $Na_V1.7$ inhibitors as analgesics, with the therapeutic goal of producing a dose-dependent attenuation of pain via pharmacological $Na_V1.7$ block that could be titrated to provide relief from pain without reproducing the human phenotype of congenital insensitivity.

$Na_V1.7$ channels are expressed on unmyelinated sensory afferents, C-fibers, at the free nerve endings, along the axon and in the cell body (*23*) where they are reported to be important in the generation of ramp currents, setting the membrane potential threshold for action potential (AP) firing (*24*) and the propagation of APs (*25*). Furthermore, $Na_V1.7$ channels have been found on sympathetic postganglionic and olfactory sensory neurons. Correspondingly, humans with homozygous SCN9A loss-of-function mutations have been diagnosed with congenital anosmia (*26*) and, in some cases, autonomic dysfunction (*27*) in addition to insensitivity to pain.

Despite a concerted effort by pharmaceutical companies to develop selective $Na_V1.7$ channel inhibitors, the clinical efficacy has been disappointing (*28*). However, it is not clear that the target has been tested comprehensively in the clinic, as no assays of target modulation were used. Therefore, the purpose of the work detailed here was to develop translational assays in nonhuman primates (NHPs) to guide anticipated human dose calculations and measure the degree of target modulation in the clinic to enable the interpretation of clinical proof-of-concept studies. Three in vivo assays were back-translated from the clinic and established in NHPs: microneurography, to assess compound effects on AP propagation (*29*) in unmyelinated afferents; threshold tracking (TT), to assess compound effects on the excitability of myelinated afferents (*30*); and an acute

[1]Merck & Co. Inc., WP-14, 770 Sumneytown Pike, P.O. Box 4, West Point, PA 19486, USA. [2]Department of Clinical Neurophysiology, Ruskin Wing, King's College Hospital, Denmark Hill, London SE5 9RS, UK.
*Corresponding author. Email: richard_kraus@merck.com

test of heat nociception using equipment used for clinical studies (*31*). A fourth assay, a functional magnetic resonance imaging (fMRI) assay to study compound effects on olfactory function, was also established in NHPs (*32*).

RESULTS

In vitro characterization of SSCI-1 and SSCI-2

Two potent and selective $Na_v1.7$ antagonists, (*R*)-5-chloro-2-fluoro-4-((4-(pyrrolidin-2-ylmethyl)amino)butyl)amino-*N*-(thiazol-2-yl) benzenesulfonamide (SSCI-1) (*33*) and 4-{[(2*S*,3*R*)-3-Amino-2-{[1-(2-aminoethyl)cyclobutyl]methyl}butyl]amino}-2,5-difluoro-*N*-(1,2,4-thiadiazol-5-yl)benzene-1-sulfonamide (SSCI-2) (*34*) (Fig. 1A), were characterized using automated patch clamp performed on the Qube (*35*). Ten-point dose-response curves were generated on human and rhesus Na_v channel isoforms stably expressed in mammalian cells. During channel pharmacology experiments, cells were held at a potential at which ~20% of the channels were inactivated. Median inhibitory concentration (IC_{50}) values of 27 ± 12 nM (n = 227) and 82 ± 23 nM (n = 4) were calculated for SSCI-1 on human and rhesus $Na_v1.7$ channels, respectively. SSCI-2 was more potent with calculated IC_{50} values of 9 ± 4 nM (n = 12) and 17 ± 3 nM (n = 3) on human and rhesus $Na_v1.7$ channels, respectively (Fig. 1B). SSCI-1 and SSCI-2 showed robust selectivity over other human and rhesus Na_v channel paralogs, with the exception of $Na_v1.2$ channels, as summarized in Table 1. The calculated IC_{50} values determined from the Qube for human and rhesus were comparable when confirmed in manual patch clamp experiments. For SSCI-1, the calculated IC_{50} values for human and rhesus channels were 66 nM (95% CI, 47 to 102 nM, n = 3) and 295 nM (95% CI, 251 to 369 nM, n = 3), respectively. For SSCI-2, the calculated IC_{50} values were 24 nM (95% CI, 17 to 36 nM, n = 3) and 62 nM (95% CI, 52 to 75 nM, n = 4) on the human and rhesus $Na_v1.7$ paralogs, respectively. We also characterized PF-05089771 on human and rhesus $Na_v1.7$ channels in manual patch clamp using the same protocol; the calculated IC_{50} values were 581 nM (95% CI, 451 to 747 nM, n = 3) and 926 nM (95% CI, 651 to 1318 nM, n = 3) for human and rhesus, respectively (Fig. 1, C and D).

To locate the binding site of SSCI-1, the compound was tested on human $Na_v1.7/1.5$ chimeras A and B using the Qube. SSCI-1 showed no activity on chimera A where residues of $Na_v1.7$ channels were replaced with residues from $Na_v1.5$ in domain IV, segments S2 and S3. Conversely, the compound inhibited sodium currents mediated by chimera B with an IC_{50} of 223 nM (95% CI, 187 to 263 nM, n = 5). In chimera B, $Na_v1.5$ highlighted residues were replaced with the corresponding $Na_v1.7$ residues (Fig. 1, E to G). These data suggest that the binding pocket for SSCI-1 resides in the voltage sensing domain IV, segments S2 and S3.

To determine whether SSCI-1 and SSCI-2 had activity on other channels and receptors, they were tested in 114 enzymatic, radioligand binding, and cellular assays at a single concentration (Eurofins). At a concentration of 10 μM, SSCI-1 did not have greater than 50% activity in any of the assays except for the choline (65%), dopamine (71%), and norepinephrine transporters (55%). SSCI-2 did not show greater than 50% activity in any of the 114 assays when tested at a single concentration of 10 μM (tables S3 and S4). The favorable in vitro profile of SSCI-1 and SSCI-2 combined with their in vivo pharmacokinetic properties (tables S5 and S6) enabled the exploration of the effects of selective $Na_v1.7$ inhibition in vivo.

SSCI-1 effects on unmyelinated nerve fiber conduction in rhesus microneurography

Microneurography is a clinical technique that uses microelectrodes to extracellularly record individual APs from peripheral nerve fibers (*36*). We adapted the methodology for NHPs to study the effects of SSCI-1 on the excitability of C-nociceptors. In healthy anesthetized rhesus macaque monkeys, the superficial peroneal nerve was exposed to record APs, using intraneural microelectrodes. The cutaneous receptive field of the superficial peroneal nerve on the foot was stimulated electrically to evoke APs. APs in individual fibers were detected and separated from background noise and from each other, based on their fixed latencies and constant conduction velocity (CV) at a stimulation rate of 0.25 Hz. When stimulated at a rate of 0.25 Hz, C-fibers settled into a stable latency of conduction and produced "flat lines" on a raster plot (the AP latency was plotted along the ordinate and the elapsed time from the start of the experiment was plotted along the abscissa). Changing the frequency of stimulation from 0.25 to 2 Hz for 3 min caused slowing of AP conduction due to the phenomenon of activity-dependent slowing (ADS) of CV. This resulted in characteristic profiles of latency increase that slowly recovered back to the baseline latency when stimulation was reverted to 0.25 Hz (*36*, *37*). C-nociceptors show the largest slowing of AP conduction during high-frequency stimulation (≥2 Hz) (*36*, *38*–*40*), resulting in ADS profiles that resemble a "shark-fin" shape, whereas the non-nociceptive C-fibers demonstrate a smaller slowing of AP conduction and have "plateau"-shaped ADS profiles.

The stability of the recordings in vehicle was established first. Each animal served as its own control. Using a protocol of 0.25-Hz stimulation with repeated 3-min periods of 2 Hz, seven C-fibers (from three animals) were studied after (intravenous) administration of vehicle for 180 min. During these vehicle experiments, only nociceptive fibers were identified. Two of the seven fibers showed block of AP conduction during 2-Hz stimulation (Table 2). This block during 2-Hz stimulation reflects either fibers shifting away from the recording electrode or an increase in stimulation threshold.

The CV and ADS profile changes of C-fibers in response to SSCI-1 treatment in eight nociceptive C-fibers and nine non-nociceptive C-fibers recorded from four animals were then evaluated. Vehicle and two doses of SSCI-1, D1 (0.4 mg/kg bolus + 0.8 mg/kg per hour infusion), and D2 (0.4 mg/kg bolus + 1.6 mg/kg per hour infusion), were tested in each animal. The vehicle was administered intravenously for 30 min followed by two doses of SSCI-1 administered intravenously sequentially for 60 min each. The mean plasma concentrations of SSCI-1 achieved are summarized in Table 2. The CV of all recorded fibers, nociceptive and non-nociceptive, was in the range of 0.56 to 1.9 m/s, typical of C-fibers. No A-fibers were isolated and analyzed. Both fiber types, nociceptive and non-nociceptive, showed a progressive increase in latency, increasing probability of spike failures, especially during 2-Hz stimulation, and eventual complete block of evoked APs by the end of the recording period in the presence of SSCI-1 (Fig. 2, A to C). Note that the apparent decrease in ADS amplitude in the presence of SSCI-1 is due to a complex interaction between the higher frequency stimulation and the increased probability of conduction failure for a given stimulus pulse due to $Na_v1.7$ inhibition (insets in Fig. 2, B and C). For the purposes of these studies, the changes in ADS amplitude reflect quantifiable changes in the excitability of the C-fibers induced by the SSCI-1 compound.

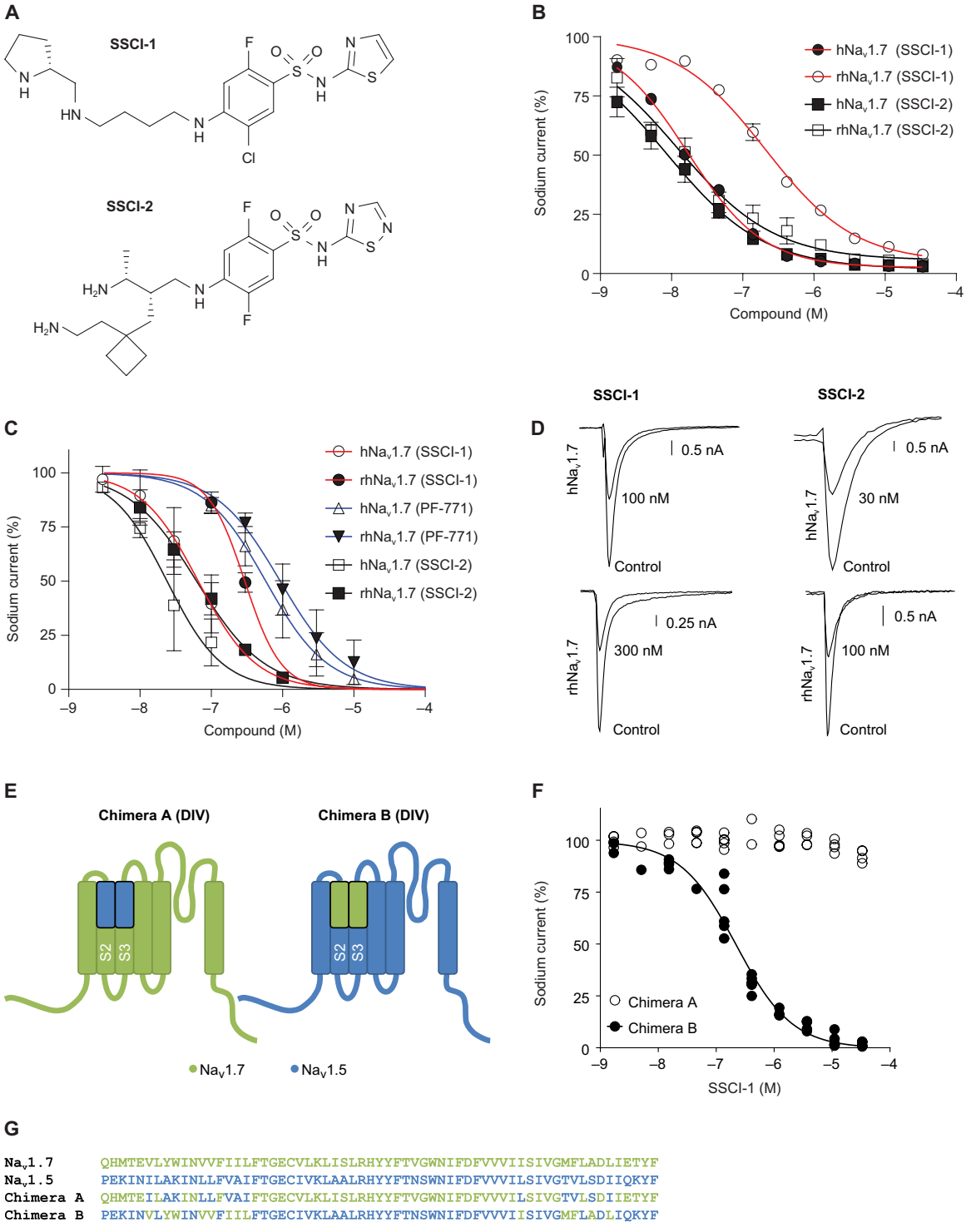

Fig. 1. In vitro characterization of SSCI-1 and SSCI-2. (**A**) Chemical structure of SSCI-1 and SSCI-2. (**B**) In vitro dose-response curves for SSCI-1 and SSCI-2 on human and rhesus Na$_v$1.7 recorded on the Qube. Representative experiments are plotted ($n = 4$ to 15). (**C**) In vitro potency of SSCI-1, SSCI-2, and clinical compound PF-05089771 on human and rhesus Na$_v$ 1.7 measured in manual patch clamp ($n = 3$ to 4). (**D**) Current traces illustrating human and rhesus Na$_v$1.7 current inhibition by SSCI-1 and SSCI-2. (**E**) Schematic drawings of domain IV (DIV) in Na$_v$1.7/1.5 chimera A and chimera B. (**F**) Dose-response curves of SSCI-1 measured on chimera A and chimera B confirming the location of the binding site in voltage sensor of domain IV. Individual experimental repeats are shown ($n = 5$). (**G**) Amino acid sequence alignments at chimeric region (DIV S1S2) highlighted in chimera A and chimera B.

Table 1. Na_v channel compound profile assessed on the Qube. EC_{50} values represent mean ± SD.

Compound	Species	$Na_v1.1$ (μM)	$Na_v1.2$ (μM)	$Na_v1.3$ (μM)	$Na_v1.4$ (μM)	$Na_v1.5$ (μM)	$Na_v1.6$ (μM)	$Na_v1.7$ (μM)	$Na_v1.8$ (μM)
SSCI-1	Human	9 ± 1.3	0.252 ± 0.088	>33	>33	>33	>33	0.027 ± 0.012	>33
		n = 10	*n* = 7	*n* = 10	*n* = 8	*n* = 9	*n* = 28	*n* = 227	*n* = 9
	Rhesus		0.089 ± 0.037		>33	>33	>33	0.082 ± 0.023	
			n = 7		*n* = 4	*n* = 4	*n* = 7	*n* = 4	
SSCI-2	Human		0.183 ± 0.037		>33	>33	>33	0.009 ± 0.004	
			n = 7		*n* = 10	*n* = 11	*n* = 6	*n* = 12	
	Rhesus		0.085 ± 0.026		>33	>33	>33	0.017 ± 0.002	
			n = 7		*n* = 6	*n* = 6	*n* = 6	*n* = 6	

Table 2. Rhesus microneurography. Compound effects on CV and ADS during C-nociceptor recordings. Blocked fibers were treated as missing and omitted from calculations. Means were calculated by first averaging fibers within a monkey and then averaging across monkeys. SE based on the standard deviation across monkeys. *N* = number of animals, *n* = number of units. SSCI-1 unbound fraction in rhesus plasma was 7.37%.

	CV (m/s) at 0.25 Hz			ADS (%) at 2 Hz			Fibers blocked (2 Hz)	Plasma exposure (μM)
	N (*n*)	Mean ± SEM	Difference from vehicle	*N* (*n*)	Mean ± SEM	Difference from vehicle		Mean ± SEM
Vehicle only experiment								
Baseline	3 (7)	0.662 ± 0.012	-	3 (7)	27.683 ± 2.11	-	0	
Vehicle 30 min	3 (7)	0.651 ± 0.013	-	3 (7)	27.313 ± 1.886	-	0	
Vehicle 60 min	3 (7)	0.646 ± 0.013	-	3 (7)	27.716 ± 1.823	-	0	
Vehicle 90 min	3 (6)	0.651 ± 0.013	-	3 (6)	24.537 ± 1.843	-	1	
Vehicle 120 min	3 (6)	0.651 ± 0.013	-	3 (6)	24.602 ± 1.918	-	1	
Vehicle 150 min	3 (6)	0.649 ± 0.013	-	3 (5)	22.96 ± 3.242	-	2	
Vehicle 180 min	3 (6)	0.652 ± 0.014	-	3 (5)	23.936 ± 2.818	-	2	
SSCI-1								
Baseline	4 (8)	0.700 ± 0.033	0.003 ± 0.004	4 (8)	27.4 ± 4.2	0.0 ± 0.5	0	
Vehicle	4 (8)	0.697 ± 0.035	-	4 (8)	27.3 ± 3.7	-	0	
SSCI-1, D1, 30 min	4 (8)	0.668 ± 0.028	−0.029 ± 0.010	4 (7)	22.2 ± 3.5	−4.7 ± 2.0	1	Not measured
SSCI-1, D1, 60 min	4 (6)	0.620 ± 0.043	−0.050 ± 0.008	3 (5)	18.9 ± 7.3	−10.7 ± 8.0	3	6.4 ± 0.47
SSCI-1, D2, 30 min	4 (5)	0.602 ± 0.041	−0.078 ± 0.015	2 (3)	20.0 ± 7.7	−8.3 ± 3.0	5	Not measured
SSCI-1, D2, 60 min	3 (4)	0.606 ± 0.035	−0.115 ± 0.029	1 (1)	13.4	−9.4	7	18.75 ± 4.1
PF-05089771								
Baseline	4 (12)	0.703 ± 0.023	0.014 ± 0.006	4 (12)	26.6 ± 1.4	0.103 ± 0.656	0	
Vehicle	4 (12)	0.72 ± 0.027	-	4 (12)	26.6 ± 1.315	-	0	
PF-05089771, 30 min	4 (12)	0.717 ± 0.028	0.0002 ± 0.002	4 (12)	27.2 ± 1.3	0.28 ± 0.2	0	Not measured
PF-05089771, 60 min	4 (12)	0.713 ± 0.029	0.004 ± 0.005	4 (12)	25.9 ± 1.7	−1.3 ± 1.2	0	110.9 ± 12.7

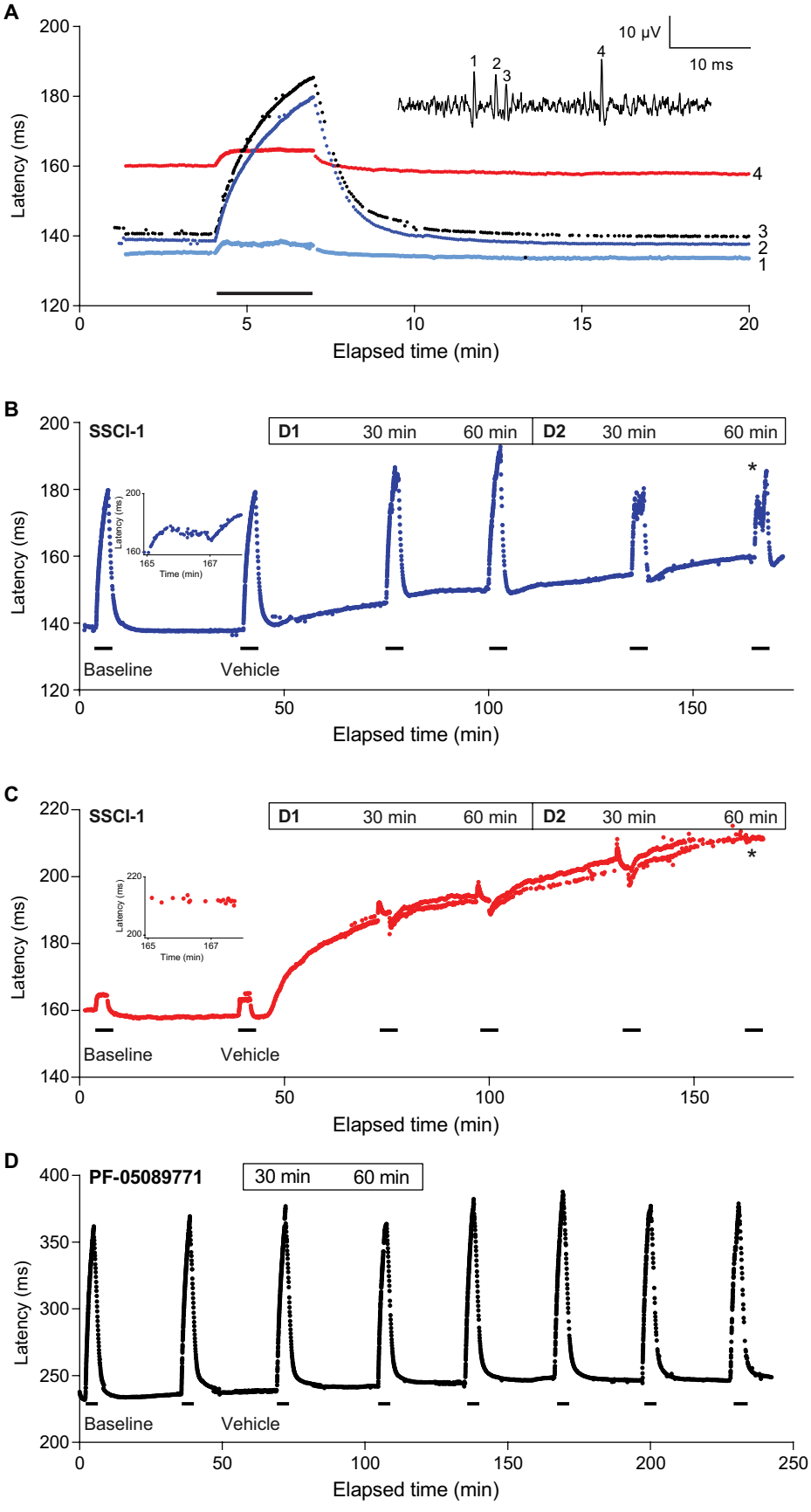

Fig. 2. Microneurography recordings showing $Na_v1.7$ modulation by SSCI-1 and PF-05089771 in peripheral C-fibers. (**A**) Modified raster plot, showing baseline evoked spike latency at 0.25-Hz stimulations and 2 Hz–induced (filled bar) ADS profiles of four units recorded. Inset: Filtered and inverted waveform after a single stimulation. (**B**) Nociceptor. Progressive increase in latency at 0.25-Hz stimulation in the presence of SSCI-1. Inset: Higher time resolution of the initial portion of the ADS curve is marked by an asterisk. (**C**) Non-nociceptor. Increase in latency at 0.25-Hz stimulation in the presence of SSCI-1. Inset: Higher time resolution of the recording is marked by an asterisk. Flip-flop phenomenon in latencies, previously described in (*61*). (**D**) Nociceptor in the presence of PF-05089771. Filled bars, 2-Hz stimulations. D1, dose 1. D2, dose 2.

We also assessed the effects of PF-05089771 on C-fibers at a dose of 4 mg/kg bolus + 5.5 mg/kg per hour infusion for 60 min. The plasma exposure achieved was equivalent to that achieved in clinical studies (*41*). Twelve nociceptive fibers and three non-nociceptive fibers were recorded from four NHPs. PF-05089771 had no effect on CV or ADS of recorded fibers measured 30 and 60 min after initiation of compound administration when compared to vehicle values (Fig. 2D, Table 2, and table S7). No block was observed. Recordings were made for an additional 60 min to check for any delayed efficacy. No run-down of response was observed over time.

The effects of SSCI-1 on CV and ADS of individual nociceptive and non-nociceptive fibers is graphed in Fig. 3 and fig. S1, respectively. Raw data are summarized in Table 2 and table S7. One non-nociceptive fiber included in table S7 could only be analyzed for changes in CV but not for changes in ADS as it tended to block during 2-Hz stimulation irrespective of the treatment. It was included in the analysis to represent all four animals that were tested with SSCI-1.

The CV of both nociceptive and non-nociceptive fibers decreased in the presence of SSCI-1. For example, the mean CV during vehicle treatment of nociceptive fibers was 0.697 ± 0.035 m/s (mean ± SEM) and decreased by ~12% to 0.606 ± 0.035 (mean ± SEM) after D2 infusion (Table 2). For non-nociceptive fibers, the decrease in CV with SSCI-1 treatment was much steeper compared to nociceptive fibers. Overall, the mean CV decreased by ~23% from 1.278 ± 0.268 (mean ± SEM) during vehicle treatment to 0.984 ± 0.328 (mean ± SEM) after D2 infusion (table S7).

Furthermore, the amplitude of ADS for nociceptive fibers was decreased in the

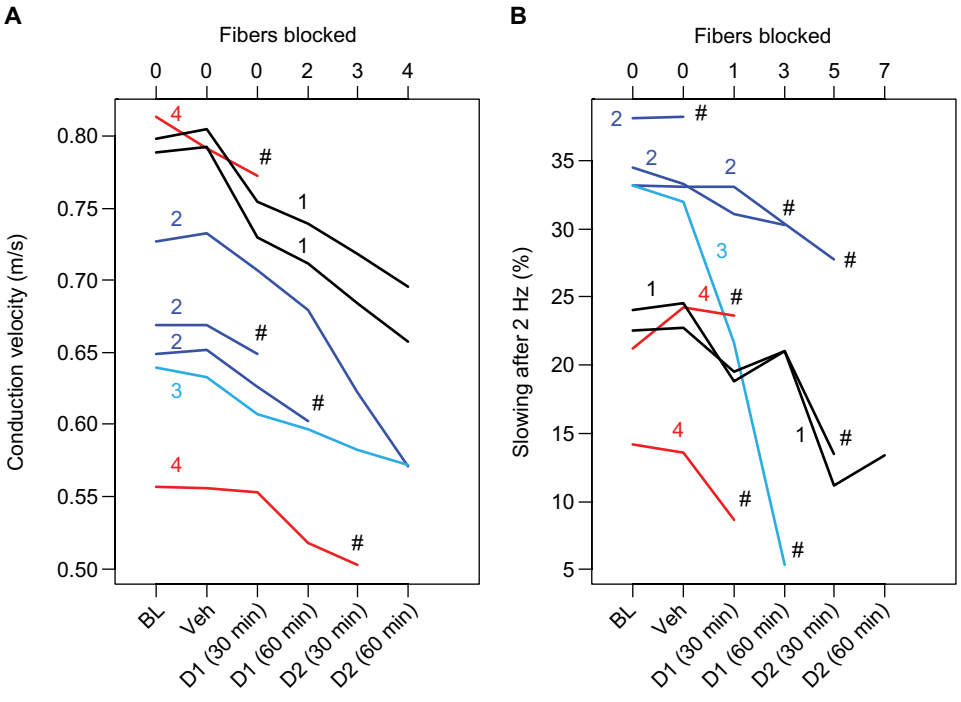

Fig. 3. SSCI-1 effects on CV and ADS for C-nociceptive fibers in rhesus microneurography. (**A**) Compound effects on CV for each of the eight nerves measured. Lines connect measurements from the same nerve. Measurements from the same animal use the same color (1, 2, 3, or 4). # indicates blocked fibers. (**B**) Compound effects on ADS. Treatment doses are indicated as D1 and D2 delivered rapidly over 3 to 5 min and the infusion completed in 60 min. BL, baseline. Veh, vehicle.

presence of SSCI-1. During vehicle infusion, the mean ADS amplitude was 27.3 ± 3.7% (mean ± SEM) decreasing to 13.4% during D2 administration. Only one fiber was recorded during D2 60-min treatment as the remaining seven fibers showed complete block of AP conduction after SSCI-1 treatment (Table 2). The block of conduction is believed to be a consequence of $Na_v1.7$ inhibition by SSCI-1, and not merely due to repeated 2-Hz stimulation, because of its disproportionate higher occurrence in the presence of SSCI-1 treatment compared to long-duration vehicle infusion or administration of PF-05089771 (Table 2). The variable time to block individual fibers after the administration of SSCI-1 likely reflects intrinsic differences in the threshold of individual fiber and/or the relative contribution of Nav1.7 to the fiber excitability.

The effect of SSCI-1 on the amplitude of ADS of non-nociceptive fibers was variable; some fibers showed minimal change, whereas others showed more noticeable decreases in ADS amplitudes. In the presence of SSCI-1, two of eight fibers showed an acceleration of CV during 2-Hz stimulation instead of the slowing observed in nociceptive fibers. The reason for acceleration of CV is unclear, but it is known that C–sympathetic fibers show a brief period of acceleration of CV during 2-Hz stimulation probably due to an enhanced I_h current secondarily to an increased concentration of extracellular potassium (*42*). Because the electrical protocol did not allow further subclassification of non-nociceptive fibers into low-threshold, cold, or sympathetic C-fibers, it is not known whether two non-nociceptive fibers that accelerated during 2-Hz stimulation in the presence of SSCI-1 were sympathetic fibers.

SSCI-1 does not affect myelinated nerve excitability as measured by TT

To determine whether SSCI-1 was affecting excitability of large myelinated sensory afferents, a second electrophysiological paradigm, TT, was used (*30*). TT of sensory nerve action potentials (SNAPs) is a minimally invasive, clinically translatable electrophysiological technique that uses surface electrodes to record compound action potentials (CAPs). The "threshold" of a CAP, the stimulus required to produce a CAP of a prespecified size, can be determined for sensory and motor fibers and generally behaves in the same way as a single unit of myelinated afferents. We determined the effects of three doses of SSCI-1 on SNAPs in anesthetized rhesus monkeys. A total of eight monkeys were tested. Some animals were used more than once across the different treatment groups (Table 3A). Robust and stable recordings were established in all animals before administration of the test compound. Ten minutes and 30 min after intravenous administration of the bolus dose of vehicle, SSCI-1, or carbamazepine (CBZ), TT measurements were recorded. There was no effect on any of the parameters tested after vehicle administration. Similarly, there were no effects on any of the parameters recorded after administration of any of the doses tested of SSCI-1. In contrast, CBZ, a nonselective sodium channel blocker, tested as a positive control (7.3 mg/kg intravenously), increased the current required to elicit an AP to 50% of the maximum, reduced the strength duration time constant, and increased the rheobase. These changes are consistent with sodium channel block (Table 3B).

SSCI-1 inhibits odorant-induced olfaction in the olfactory bulb of rhesus monkeys, measured by fMRI

Humans with loss-of-function mutations in $Na_v1.7$ are anosmic (*26*), suggesting that odor detection could be used as a target modulation biomarker for $Na_v1.7$ inhibitors. An fMRI technique, measuring cerebral blood volume (CBV) with a contrast agent to assess odor-induced olfaction in the olfactory bulb (OB) of NHPs, was previously developed (*32*). CBV fMRI is sensitive to neural activation–induced CBV increase (*43*). The effect of the compound on odorant-induced olfaction in the OB of rhesus monkeys was measured to determine modulation of olfaction in rhesus monkeys. Vehicle and five different doses of SSCI-1 were tested in 13 rhesus macaque monkeys. Some animals were used more than once across the different treatment groups (table S1).

Robust odor-induced olfaction was observed by fMRI in the OB of all NHPs tested. Measured color-encoded fMRI activations in the OB induced by the odor stimulation in the three fMRI slices encompassing the OB from one animal are illustrated (Fig. 4, A to C). The strength of 10 fMRI responses was quantified by averaging the

Table 3. Rhesus TT. (**A**) Group designation, SSCI-1 and CBZ. (**B**) Compound effects. Values are means ± SEM. SSCI-1 unbound fraction in rhesus plasma was 7.37%.

A

Study	Group no.	Number of animals	Total dose (mg/kg)	Treatment protocol	Plasma concentration (μM) 60 min after dosing
Vehicle	1	7	0	30% captisol 2 ml bolus + 6 ml/ hour infusion	-
SSCI-1	2	3	1.34	0.49 mg/kg bolus + 0.85 mg/kg per hour infusion	7.76 ± 0.52
	3	3	4.02	1.47 mg/kg bolus + 2.55 mg/kg per hour infusion	36.4 ± 5.23
	4	3	12.06	4.41 mg/kg bolus + 7.65 mg/kg per hour infusion	104 ± 25.7
CBZ	5	7	7.3	5 mg/kg bolus + 2.3 mg/kg per hour infusion	30.8 ± 3.4

B

Study	Total dose (mg/kg)	Time of reading	Stimulus (mA) for 50% max. response	Strength duration time constant	Rheobase (mA)	Stimulus response slope
Vehicle		Baseline	1.38 ± 0.17	0.42 ± 0.02	0.73 ± 0.1	4.2 ± 0.38
		30 min	1.45 ± 0.15	0.4 ± 0.02	0.78 ± 0.09	3.71 ± 0.33
SSCI-1	1.34	Baseline	1.45 ± 0.35	0.43 ± 0.03	0.75 ± 0.13	3.47 ± 0.48
		30 min	1.47 ± 0.32	0.39 ± 0.01	0.82 ± 0.17	3.89 ± 0.23
	4.02	Baseline	1.49 ± 0.28	0.47 ± 0.05	0.76 ± 0.16	4.41 ± 0.5
		30 min	1.55 ± 0.28	0.44 ± 0.04	0.83 ± 0.17	3.28 ± 0.55
	12.06	Baseline	1.07 ± 0.09	0.47 ± 0.04	0.55 ± 0.06	4.21 ± 0.64
		30 min	1.19 ± 0.08	0.42 ± 0.04	0.64 ± 0.06	4.2 ± 0.67
CBZ	7.3	Baseline	1.37 ± 0.17	0.46 ± 0.04	0.70 ± 0.10	2.92 ± 0.31
		30 min	1.51 ± 0.18**	0.42 ± 0.03**	0.81 ± 0.11**	3.25 ± 0.32

**$P < 0.001$, paired t test 30 min reading versus baseline.

amplitudes of fMRI signals during the stimulation period for each experiment. Robust olfactory responses to the odor stimulations in the OB were measured throughout a 2-hour period (Fig. 4D). No vehicle effects were observed. The highest dose (24.12 mg/kg) of SSCI-1 substantially suppressed the olfactory responses to the applied odor stimulations (Fig. 4E).

The inhibition of SSCI-1/vehicle on the olfactory activation was calculated as percentage change of the fMRI response strength from the average response strength before compound delivery. The temporal profiles from all the experiments of each treatment group were averaged, and dose-dependent effects are summarized in Fig. 4F.

No inhibition was observed [analysis of variance (ANOVA): $F_{9,50} = 1.7$, $P = 0.1$] after intravenous administration of vehicle. In contrast, dose-dependent inhibition in the fMRI responses induced by the olfactory stimulus was observed after administration of SSCI-1 (ANOVA for the 1.34 mg/kg group: $F_{9,40} = 4.1$, $P = 8.1 \times 10^{-4}$; for the 2.68 mg/kg group: $F_{9,30} = 12.6$, $P = 5.4 \times 10^{-8}$; for the 4.02 mg/kg group: $F_{9,30} = 9.5$, $P = 1.2 \times 10^{-6}$; for the 12.06 mg/kg group: $F_{9,40} = 31.8$, $P = 1.7 \times 10^{-15}$; for the 24.12 mg/kg group: $F_{9,40} = 31.9$, $P = 1.6 \times 10^{-15}$). For the animals treated with the two highest doses (12.06 mg/kg and 24.12 mg/kg), there was statistically significant inhibition of the response at all time points measured after initiation of the SSCI-1 infusion (Student's t test, $P < 0.01$ with Bonferroni correction). The highest dose of SSCI-1 (24.12 mg/kg) achieved almost complete inhibition of OB activation induced by the odorant. The plasma concentrations of SSCI-1 60 min after initiating the infusion in different treatment groups are listed in table S1.

The effects of the clinical compound PF-05089771 on the odor-induced stimulation of olfaction in the OB of NHPs by fMRI were also determined (Fig. 4F). A dose of 4 mg/kg (bolus) + 5.5 mg/kg per hour (infusion) was selected to achieve plasma exposure comparable to recently reported exposures in clinical studies (*41*). PF-05089771

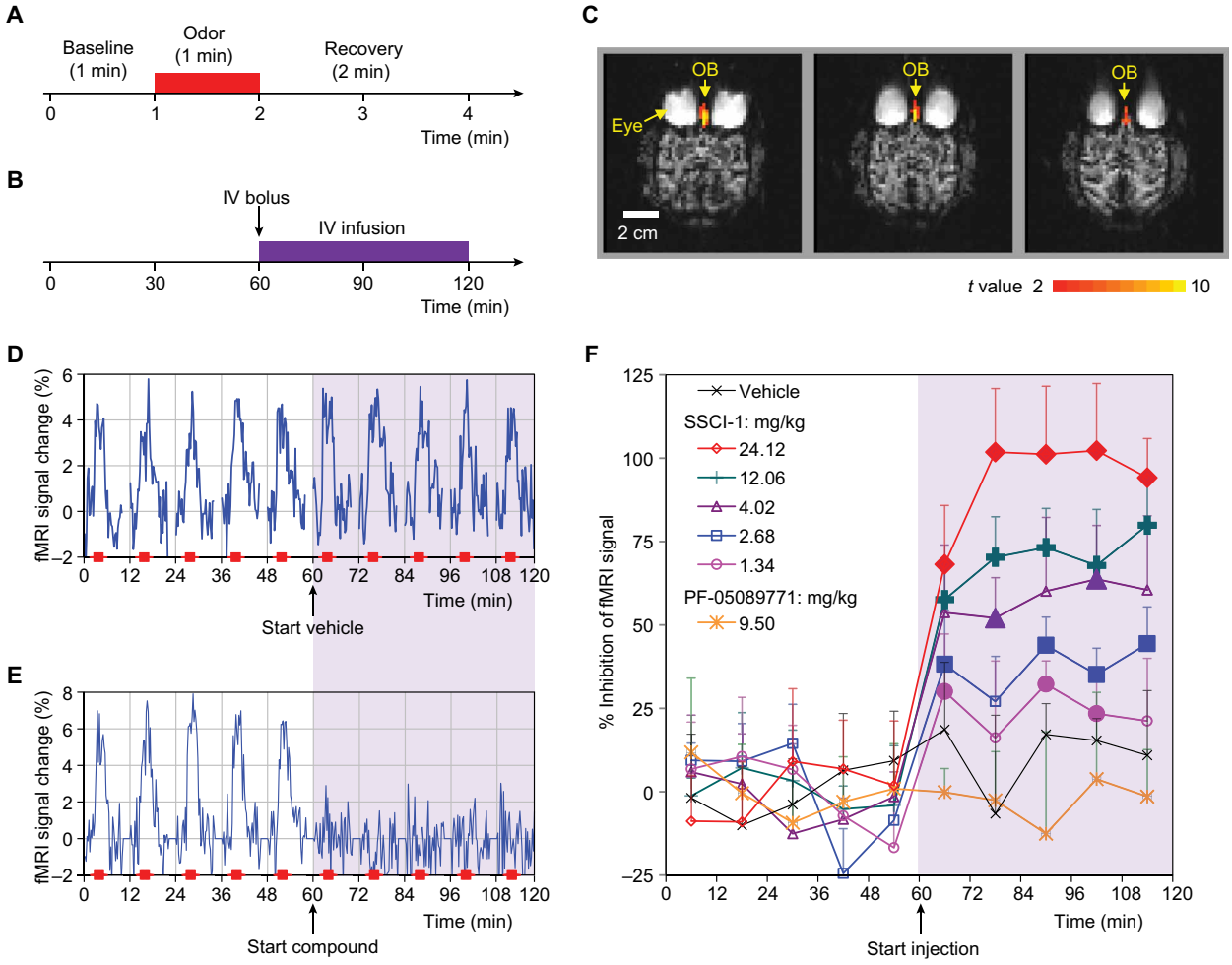

Fig. 4. Effects of SSCI-1 and PF-05089771 on odor-induced olfaction in the OB of NHPs. (**A**) Odor stimulation paradigm for each fMRI measurement, including a baseline (1 min), odor delivery (red bar, 1 min), followed by recovery (2 min) for a total of 4 min for each fMRI measurement. (**B**) Thirty fMRI measurements were performed for each animal during a 2-hour experiment session. The intravenous (IV) delivery of the vehicle or compounds was started at 1 hour with bolus and followed by continuous 1-hour infusion as indicated by the purple bar. (**C**) Odor-induced olfaction in the OB. Odor-induced fMRI activations are shown in the consecutive three 1.8-mm axial slices where OB is located. Yellow, strong; red, weak. (**D**) The time course of fMRI signals in the OB from a single NHP in the vehicle group. Red bars, 1-min odor stimuli. Purple-shaded region indicates the vehicle injection. (**E**) The time course of fMRI signals in the OB from a single NHP in the SSCI-1 group with the highest dose. Red bars, 1-min odor stimuli. (**F**) SSCI-1 and PF-05089771 effects on odor-induced olfaction. Averaged temporal profiles of the inhibition of the olfaction for all study groups (mean ± SEM). The enlarged/filled signs during the delivery (purple-shaded area) indicate times when a statistically significant difference ($P < 0.01$ with Bonferroni correction) from pretreatment was reached.

showed no inhibition of odor-induced olfaction in the OB of NHPs (ANOVA: $F_{9,40} = 0.5$, $P = 0.9$); the mean plasma concentration achieved was 107.4 ± 23.6 μM (mean ± SE).

SSCI-1 and SSCI-2 inhibit withdrawal responses to noxious heat in rhesus monkeys

A clinically translatable behavioral assay that measures heat-induced pain-like behaviors in healthy NHPs was previously described (*31*). The effects of SSCI-1 and SSCI-2 and a single dose of morphine (3 mg/kg, subcutaneously) were determined. Vehicle-treated animals showed a temperature-dependent increase in arm withdrawal responses. A temperature stimulus of 44°C produced no behavioral response. After application of a 46°C stimulus, withdrawal responses became apparent and increased in frequency after application of the 48° and 50°C stimuli. After a single subcutaneous dose of 20 mg/kg of SSCI-1, nociceptive behaviors were inhibited (Fig. 5A). A two-factor (temperature × group) two-way repeated measures ANOVA indicated significant main effects of temperature ($F_{3,18} = 71.0$, $P < 0.0001$) and treatment group ($F_{2,12} = 38.4$, $P < 0.0001$), and a significant interaction of temperature and treatment group ($F_{6,36} = 13.8$, $P < 0.0001$). SSCI-1 (20 mg/kg) significantly inhibited arm-withdrawal response induced by noxious temperature stimuli of 46°, 48°, and 50°C ($P < 0.05$, $P < 0.0001$, and $P < 0.001$, respectively, Dunnett's multiple comparisons). The morphine control group also produced a significant reduction of response at these temperatures ($P < 0.01$ for 46°C and $P < 0.0001$ for 48° and 50°C, Dunnett's multiple comparisons). Higher doses of SSCI-1 were not tested owing to the limited solubility of the compound.

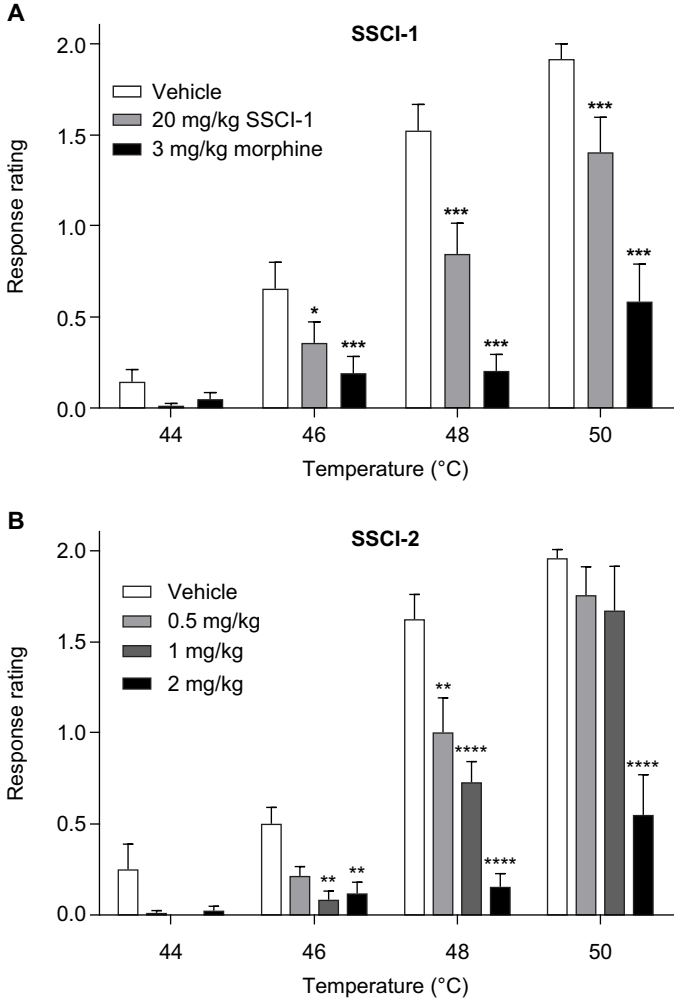

Fig. 5. Rhesus thermode study. (**A**) Effect of SSCI-1 and morphine on noxious heat–evoked pain behaviors. (**B**) Dose-dependent effect of SSCI-2 on noxious heat–evoked pain behaviors ($P < 0.05$ to $P < 0.0001$, two-way ANOVA, Dunnett's multiple comparisons). *$P < 0.05$; **$P < 0.01$; ***$P < 0.001$; ****$P < 0.0001$ ($N = 7$ for both experiments; bars represent mean ± SEM).

To demonstrate that selective Nav1.7 inhibitors could produce dose-dependent effects, SSCI-2 was also tested (Fig. 5B). This compound has improved potency and pharmacokinetic properties. Three doses of SSCI-2 (0.5, 1, or 2 mg/kg) or vehicle were injected subcutaneously and behavior assessments were performed 2 hours after dosing at T_{max}. SSCI-2 inhibited the arm-withdrawal response induced by noxious temperature stimuli of 46°, 48°, and 50°C (two-way repeated measures ANOVA with Dunnett's multiple comparisons). This two-factor (temperature × dose) ANOVA indicated significant main effects of temperature ($F_{3,18} = 55.6$, $P < 0.0001$) and dose ($F_{3,18} = 21.7$, $P < 0.0001$), and a significant interaction of temperature and dose ($F_{9,54} = 13.1$, $P < 0.0001$). Dunnett's multiple comparisons revealed a significant effect of 1 and 2 mg/kg at 46°C ($P < 0.01$); 0.5, 1, and 2 mg/kg at 48°C ($P < 0.0001$); and 2 mg/kg at 50°C ($P < 0.0001$). The plasma exposures measured for SSCI-1 and SSCI-2 are listed in table S2. We were unable to test PF-05089771 in this assay because target exposures equivalent to those achieved in the clinic could not be achieved by subcutaneous dosing.

DISCUSSION

In 2006, $Na_v1.7$ emerged as a promising target for future pain therapeutics (*20*). Even with substantial investment from many biopharmaceutical companies to identify selective $Na_v1.7$ channel inhibitors, robust analgesic efficacy in humans with either small- or large-molecule therapeutics is yet to be reported. Pfizer has made the most progress, assessing the effects of PF-05089771 (*44*) in patients with dental pain, painful diabetic neuropathy, thermode-evoked pain, and erythromelalgia (*41*, *45*). Despite success in identifying compounds that are pharmacologically selective for $Na_v1.7$ over other paralogs in vitro (*46*), the clinical efficacy data were disappointing compared to what was anticipated based on the loss-of-function phenotype. In patients with diabetic neuropathy, PF-05089771 (150 mg BID) showed a trend toward a reduction in pain scores and an improvement in sleep rating scores when compared to placebo. However, these effects were not statistically significant (*45*). In people with third molar extraction pain, 50 to 1600 mg did show a statistical improvement in pain scores compared to placebo, but the magnitude of relief was half that of the positive control ibuprofen (*45*). Similarly, in people with erythromelalgia, only a subset of patients obtained clinically meaningful relief from evoked pain after a single administration of 1600 mg of PF-05089771 (*41*). Furthermore, PF-05089771 (300 mg) alone or concomitantly with pregabalin did not demonstrate analgesic properties in a battery of pain models in healthy subjects (*47*). These data have led some to conclude that inhibition of $Na_v1.7$ channels by a small-molecule inhibitor is insufficient to provide adequate pain relief in patients (*45*). However, Pfizer did not demonstrate that the doses of PF-05089771 used were sufficient to inhibit $Na_v1.7$ channels in vivo. Without demonstration of target modulation by PF-05089771 in these studies, it is difficult to draw definitive conclusions, and it may be that the doses were too low to fully test the mechanism. Targeted plasma exposures in Pfizer's early clinical development program were based on in vitro IC_{50} values of PF-05089771 derived from electrophysiological studies conducted in both transfected cell lines and human DRG neurons (*25*, *48*). Choosing a human dose based on multiples over an in vitro IC_{50} assumes equivalent target modulation in vivo. This may not be the case for a number of reasons, including protein binding, distribution of unbound compound to the site of action, and the pulse protocol used to measure in vitro potency of state-dependent compounds not being relevant to the in vivo situation. In our electrophysiology paradigm, selected based on in vivo–in vitro correlations, PF-05089771 appeared to be a weak blocker of rhesus $Na_v1.7$ channels (IC_{50} of 926 nM). Furthermore, it was found to be highly protein bound (99.9%), making calculation of the unbound free fraction challenging.

Therefore, calculating an anticipated human efficacious dose using IC_{50} values calculated from in vivo preclinical assays of efficacy and target modulation should improve the predictive value of the calculations. Furthermore, if these assays are vertically translatable to the clinic, the ability to understand target modulation in people should be improved, allowing target doses to be adjusted accordingly to ensure that the mechanism has been explored maximally. Thus, a number of assays were explored to determine whether they were sensitive to $Na_v1.7$ inhibition and whether efficacy or target modulation could be quantified to improve anticipated human dose calculations. The assays used were prioritized based on the human loss-of-function phenotype and whether they could be used in clinical studies. Once the assays were established in rhesus macaque primates, we tested two selective $Na_v1.7$ inhibitors potent at inhibiting

$Na_v1.7$ channels in rhesus as well as humans. SSCI-1 and SSCI-2 are 1000-fold selective for $Na_v1.7$ channels over all other human sodium channel isoforms measured except $Na_v1.2$. The in vitro selectivity profile of SSCI-1 and SSCI-2 combined with their pharmacokinetic profiles made them ideal tools to validate the in vivo assays and explore the biology of $Na_v1.7$ inhibitors as a high degree of in vivo target modulation could be achieved. Like other arysulfonamides (*46*), SSCI-1 and SSCI-2 interact with the voltage sensor in domain IV, a site distinct from the binding sites of local anesthetics and tetrodotoxin. A similar binding pocket has been previously described in mutagenesis studies using the state-dependent inhibitor PF-04856264 (*46*) and was confirmed by an x-ray crystal structure of a chimeric human $Na_v1.7$ voltage sensor domain IV in complex with an arylsulfonamide (*49*).

Microneurography was used to record electrically evoked APs generated in unmyelinated afferents of rhesus monkeys to study the role of $Na_v1.7$ channels in AP propagation as well as to identify and measure end points that could be used as biomarkers of target modulation in the clinic. Similar types of C-fibers are present in rodents, monkeys, and humans, making this technique highly translational (*50*). CV and ADS at 2-Hz stimulation frequency were measured under control conditions and after vehicle or SSCI-1 administration. SSCI-1 dose-dependently decreased CV and reduced the average magnitude of ADS during 2-Hz stimulation. At higher doses, most recorded fibers displayed complete block of AP conduction in the presence of SSCI-1. The effects of higher stimulus intensities were not explored in these studies. Analysis of our acute recordings with higher time resolution demonstrated an inability of recorded fibers to regularly follow electrical stimulation at 2 Hz in the presence of SSCI-1. This overall impairment of conduction resulted in a decrease of the ADS amplitude. These results are consistent with the attenuation of pain behaviors reported with SSCI-1 in the thermode assay and a decrease in the olfaction-induced fMRI signal.

In several fibers, the block of conduction was most noticeable with SSCI-1 at 2-Hz stimulation, whereas these same fibers were able to conduct APs at lower frequency (0.25 Hz). This may be a result of a complex interaction of higher-frequency stimulation and state-dependent $Na_v1.7$ inhibition induced by SSCI-1 (*51*). Spontaneous firing of APs in C-fibers in painful conditions is suggested to occur in the 0.5- to 10-Hz range (*52*, *53*). Hence, a preferential block of conduction during higher rates of stimulation may be physiologically beneficial in selectively blocking painful signaling. A consequence of attenuating conduction in unmyelinated nociceptive fibers is an inhibition of nociception observed in the thermode assay. A block of conduction by SSCI-1 in non-nociceptive fibers was also observed, which could potentially affect the activity of cold, low-threshold, or sympathetic efferent fibers. However, responses to cold stimuli were not assessed in the current studies to explore this possibility. The effect of SSCI-1 on AP propagation appears to be limited to unmyelinated fibers, given the lack of effect on large myelinated sensory afferents observed in the TT paradigm. This is consistent with the reports of people with loss-of-function mutations having normal thresholds to stimuli conducted by large myelinated afferents.

These data suggest that inhibition of $Na_v1.7$ channels in rhesus C-nociceptors leads to changes in neuronal excitability and/or conductivity and can even block the propagation of APs in this fiber class completely at stimulus intensities sufficient to cause AP propagation before $Na_v1.7$ channel inhibition. Failure of conduction of APs from peripheral C-nociceptors would result in no presynaptic potential and no associated release of neurotransmitters to activate second-order nociceptive neurons in the spinal cord. It was previously reported that postsynaptic potentials could not be recorded in the olfactory system of $Na_v1.7$-deficient mice, even when the odor initiated an AP in the olfactory sensory neurons (*26*). These data suggest that peripheral block of $Na_v1.7$ is sufficient to inhibit afferent input via C-fibers and that inhibition of $Na_v1.7$ channels in the CNS may not be required to elicit analgesia.

Humans with loss of function of $Na_v1.7$ experience anosmia (*20*, *26*). $Na_v1.7$ is the predominant sodium channel in rodent olfactory sensory neurons (*54*) and dysfunction of the olfactory system has been described in $Na_v1.7$ knockout mice (*26*, *54*, *55*). SSCI-1 prevented activation of the OB after odor application to the nasal cavity in the rhesus fMRI study. The inhibitory effect was dose dependent; lower plasma concentrations of SSCI-1 only partially inhibited OB activation. Given the microneurography data, it is conceivable that APs initiated in rhesus olfactory neurons fail to propagate and generate presynaptic potentials (*25*). Because SSCI-1 does not cross the blood-brain barrier effectively, it is less likely that SSCI-1 is having a direct inhibitory effect on postsynaptic neurons in the OB; SSCI-1 concentration measured in the CNS was ≤1% of the unbound concentration in plasma (table S6), suggesting that pharmacological inhibition of peripheral $Na_v1.7$ channels is sufficient to affect odor detection.

Subcutaneously administered SSCI-1 and SSCI-2 dose-dependently inhibited withdrawal responses to noxious heat. About 50% inhibition was achieved at 46° and 48°C thermal stimuli at a SSCI-1 plasma concentration of 7.7 μM. When corrected for binding to rhesus plasma proteins, unbound concentration corresponded to about sevenfold the Qube in vitro rhesus $Na_v1.7$ IC_{50} value. A smaller reduction of the response to the 50°C stimulus was observed. Because higher plasma concentrations of SSCI-1 could not be achieved after subcutaneous administration, SSCI-2 was used to assess the effects of increased $Na_v1.7$ channel inhibition in this assay. For SSCI-2, a higher plasma concentration of 12.9 μM was achieved; the unbound concentration was ~112-fold over the Qube rhesus $Na_v1.7$ IC_{50}. At this exposure, near-complete block of the noxious thermal behavioral withdrawal response to 48°C was observed. The suppression of the withdrawal response to 50°C was incomplete. However, it was comparable to morphine at clinically used exposures.

For the olfaction and microneurography assays, SSCI-1 could be administered intravenously, enabling higher plasma exposures. In the microneurography assay, conduction block by SSCI-1 occurred in seven of eight recorded C-nociceptive fibers at a plasma concentration of 18.7 μM, and SSCI-1 caused almost complete inhibition of the response in the fMRI olfaction study when the measured plasma concentration was 169 μM. The effects of SSCI-1 and SSCI-2 were dose dependent; the assays described suggest that dose-dependent attenuation of pain via pharmacological $Na_v1.7$ block is possible. Most affected humans with SCN9A loss-of-function mutations are homozygous with heterozygous mutations often conferring no phenotype (*56*).

For PF-05089771, an in vitro IC_{50} of 926 nM on rhesus $Na_v1.7$ channels was determined and was used to calculate exposures required to be comparable to those achieved in the published clinical studies. However, at these concentrations, no effects were observed in our NHP microneurography and fMRI studies. The compound was highly protein bound (99.9%) such that the free plasma concentration was below the rhesus $Na_v1.7$ in vitro IC_{50}, explaining the

lack of efficacy in our NHP assays. It may also explain why only moderate pharmacodynamic effects were observed in the clinical studies. Human $Na_v1.7$ in vitro IC_{50} values of 11 and 10 μM were reported previously for channels in the inactivated state and resting state, respectively (*25*).

There are several limitations to these studies. The primary goal of the microneurography studies was to establish a translatable means to study the pharmacological effects of $Na_v1.7$ inhibitors in peripheral C-fibers in vivo. Therefore, to keep the experimental protocols simple and efficient, the typical pause protocol was not used to further classify nociceptive fibers into mechanosensitive afferents (type 1A) or mechano-insensitive afferents (type 1B), C-thermoreceptors (type 2), low threshold C-mechanoreceptors (type 3), or sympathetic (type 4) fibers (*42*, *57*). Furthermore, the receptive field of recorded neurons was not tested for responses to mechanical or thermal stimulation in addition to the electrical stimulation. Thus, the C-fibers recorded can only be categorized as nociceptive or non-nociceptive. Electrical stimulation intensity was not increased after compound application, so apparent conduction block cannot be differentiated from a possible increased threshold for AP firing. There was inhibition of non-nociceptive fibers, possibly including sympathetic fibers. Although no obvious sympathetic effects were observed in the reported studies, follow-up work is in progress to further explore the effects on cardiovascular parameters of potential inhibition of sympathetic neurons looking at end points in addition to heart rate and blood pressure.

Furthermore, unlike the other methodologies used, fMRI of the OB has not been performed routinely in humans. Because of the size and location of the OB in humans, it may be challenging to transfer this methodology to humans to demonstrate pharmacological modulation. Simple bedside testing of olfaction, for example, using "sniffin"-sticks (*58*), could be used as an alternative in the clinic.

In conclusion, sufficient pharmacological in vivo block of $Na_v1.7$ channels in NHPs inhibits nociceptive afferent input and activation of the OB by an odorant measured. Compared to using in vitro data alone, using in vivo data of target modulation and efficacy should improve anticipated human dose calculations for phase 1 clinical trials. Furthermore, these same assays could be used in human volunteers to assess $Na_v1.7$ target modulation to further refine doses for phase 2A and help with the interpretation of clinical data from patients.

MATERIALS AND METHODS

Study design

This study was designed to assess the effects of pharmacological inhibition of $Na_v1.7$ channels in NHPs. Small-molecule inhibitors of $Na_v1.7$ were identified using automated patch clamp and chosen based on potency, selectivity, and pharmacokinetic properties. The effects of lead compounds were tested in NHP assays. These assays included C-fiber microneurography, TT, heat responsivity, and olfactory fMRI.

Because of the limited availability of NHPs for the anesthetized studies, C-fiber microneurography, TT, and olfactory fMRI, they were performed in a nonblinded fashion with an adaptive design to reduce the number of animals required. A decision on futility was made after each dose, with numbers of animals being increased only when an effect was observed and numbers were increased to a achieve a sample size sufficient to achieve statistical significance based on previous studies (*31*, *59*). In addition, for microneurography, animals were randomly assigned from a pool of animals slated to be euthanized. For heat responsivity, experiments were performed and analyzed blind. The number of replicates used in each study for each treatment is indicated. All collected data are shown. Principles from the *Guide for the Care and Use of Laboratory Animals*, National Institute of Health, and U.S. Department of Agriculture were followed, and all protocols were approved by the Institutional Animal Care and Use Committee of Merck & Co. Inc., Kenilworth, NJ, USA.

Statistical analysis

Rhesus microneurography

Estimates of mean CV and ADS of recorded fibers in each treatment group and changes from vehicle were obtained by averaging fibers for each animal followed by averaging animals within the group. Blocked fibers were treated as missing for these calculations. Estimates are provided as mean ± SE in Table 2. Although *P* values are not provided, as is consistent with current statistical thinking (*60*) for nonconfirmatory experiments, estimates of mean differences from vehicle more than 2 SEs from 0 suggest good evidence of a nonzero treatment difference in the population.

Rhesus TT

Data were averaged to calculate the mean ± SEM for each parameter before and after compound administration. A one-way ANOVA was performed to test for effects of treatment followed by a pairwise *t* test with Bonferroni correction to compare the effect of drug treatment versus the baseline readings.

Rhesus fMRI

The effect of vehicle or SSCI-1 on the olfaction was examined by a one-way repeated measures ANOVA by comparing the amplitudes of fMRI activations from the 10 equivalent responses. If statistical significance ($P < 0.05$) was observed, the statistical significance between the amplitudes of fMRI activations after initiating the compound infusion and the amplitudes of fMRI activations immediately before the compound treatment was tested by one-tailed Student's *t* test (paired) after Bonferroni corrections for multiple comparisons were applied.

Rhesus thermode assay

Two-factor (temperature and treatment group) two-way repeated measures ANOVAs were performed to test for main effects of temperature and group, as well as interactions between these factors, followed by Dunnett's multiple comparisons post hoc test to compare drug treatment versus the vehicle group at each temperature.

SUPPLEMENTARY MATERIALS

stm.sciencemag.org/cgi/content/full/13/594/eaay1050/DC1
Materials and Methods
Fig. S1. Rhesus microneurography.
Table S1. Rhesus fMRI group designation.
Table S2. Rhesus heat responsivity, dose, and plasma concentrations.
Table S3. Selectivity of SSCI-1.
Table S4. Selectivity of SSCI-2.
Table S5. Pharmacokinetic properties of SSCI-1 and SSCI-2 administered intravenously and subcutaneously in NHPs.
Table S6. Concentrations of SSCI-1 in plasma, brain, and CSF after intravenous infusion in NHPs.
Table S7. Rhesus microneurography.
Data file S1. Rhesus microneurography (Microsoft Excel format).
Data file S2. Rhesus TT (Microsoft Excel format).
Data file S3. Rhesus fMRI (Microsoft Excel format).
Data file S4. Rhesus thermode (Microsoft Excel format).

View/request a protocol for this paper from *Bio-protocol*.

REFERENCES AND NOTES

1. A. E. Dubin, A. Patapoutian, Nociceptors: The sensors of the pain pathway. *J. Clin. Invest.* **120**, 3760–3772 (2010).
2. G. R. Tibbs, D. J. Posson, P. A. Goldstein, Voltage-gated ion channels in the PNS: Novel therapies for neuropathic pain? *Trends Pharmacol. Sci.* **37**, 522–542 (2016).
3. S. G. Waxman, G. W. Zamponi, Regulating excitability of peripheral afferents: Emerging ion channel targets. *Nat. Neurosci.* **17**, 153–163 (2014).
4. A. S. Yekkirala, D. P. Roberson, B. P. Bean, C. J. Woolf, Breaking barriers to novel analgesic drug development. *Nat. Rev. Drug Discov.* **16**, 545–564 (2017).
5. A. I. Basbaum, D. M. Bautista, G. Scherrer, D. Julius, Cellular and molecular mechanisms of pain. *Cell* **139**, 267–284 (2009).
6. L. A. McDermott, G. A. Weir, A. C. Themistocleous, A. R. Segerdahl, I. Blesneac, G. Baskozos, A. J. Clark, V. Millar, L. J. Peck, D. Ebner, I. Tracey, J. Serra, D. L. Bennett, Defining the functional role of $Na_V1.7$ in human nociception. *Neuron* **101**, 905–919.e8 (2019).
7. S. D. Dib-Hajj, T. R. Cummins, J. A. Black, S. G. Waxman, From genes to pain: Na_v 1.7 and human pain disorders. *Trends Neurosci.* **30**, 555–563 (2007).
8. S. D. Dib-Hajj, T. R. Cummins, J. A. Black, S. G. Waxman, Sodium channels in normal and pathological pain. *Annu. Rev. Neurosci.* **33**, 325–347 (2010).
9. J. P. H. Drenth, S. G. Waxman, Mutations in sodium-channel gene *SCN9A* cause a spectrum of human genetic pain disorders. *J. Clin. Invest.* **117**, 3603–3609 (2007).
10. Y. Yang, M. A. Mis, M. Estacion, S. D. Dib-Hajj, S. G. Waxman, $Na_V1.7$ as a pharmacogenomic target for pain: Moving toward precision medicine. *Trends Pharmacol. Sci.* **39**, 258–275 (2018).
11. I. E. Dick, R. M. Brochu, Y. Purohit, G. J. Kaczorowski, W. J. Martin, B. T. Priest, Sodium channel blockade may contribute to the analgesic efficacy of antidepressants. *J. Pain* **8**, 315–324 (2007).
12. B. T. Priest, G. J. Kaczorowski, Blocking sodium channels to treat neuropathic pain. *Expert Opin. Ther. Targets* **11**, 291–306 (2017).
13. P. L. Sheets, C. Heers, T. Stoehr, T. R. Cummins, Differential block of sensory neuronal voltage-gated sodium channels by lacosamide [(2*R*)-2-(acetylamino)-*N*-benzyl-3-methoxypropanamide], lidocaine, and carbamazepine. *J. Pharmacol. Exp. Ther.* **326**, 89–99 (2008).
14. S. Y. Wang, J. Calderon, G. Kuo Wang, Block of neuronal Na^+ channels by antidepressant duloxetine in a state-dependent manner. *Anesthesiology* **113**, 655–665 (2010).
15. D. E. Moulin, A. Boulanger, A. J. Clark, H. Clarke, T. Dao, G. A. Finley, A. Furlan, I. Gilron, A. Gordon, P. K. Morley-Forster, B. J. Sessle, P. Squire, J. Stinson, P. Taenzer, A. Velly, M. A. Ware, E. L. Weinberg, O. D. Williamson, Pharmacological management of chronic neuropathic pain: Revised consensus statement from the Canadian Pain Society. *Pain Res. Manag.* **19**, 328–335 (2014).
16. A. M. Waszkielewicz, A. Gunia, K. Słoczyńska, H. Marona, Evaluation of anticonvulsants for possible use in neuropathic pain. *Curr. Med. Chem.* **18**, 4344–4358 (2011).
17. S. D. Dib-Hajj, Y. Yang, J. A. Black, S. G. Waxman, The $Na_V1.7$ sodium channel: From molecule to man. *Nat. Rev. Neurosci.* **14**, 49–62 (2013).
18. C. A. Ahern, J. Payandeh, F. Bosmans, B. Chanda, The hitchhiker's guide to the voltage-gated sodium channel galaxy. *J. Gen. Physiol.* **147**, 1–24 (2016).
19. M. de Lera Ruiz, R. L. Kraus, Voltage-gated sodium channels: Structure, function, pharmacology, and clinical indications. *J. Med. Chem.* **58**, 7093–7118 (2015).
20. J. J. Cox, F. Reimann, A. K. Nicholas, G. Thornton, E. Roberts, K. Springell, G. Karbani, H. Jafri, J. Mannan, Y. Raashid, L. Al-Gazali, H. Hamamy, E. M. Valente, S. Gorman, R. Williams, D. P. McHale, J. N. Wood, F. M. Gribble, C. G. Woods, An SCN9A channelopathy causes congenital inability to experience pain. *Nature* **444**, 894–898 (2006).
21. D. L. H. Bennett, C. G. Woods, Painful and painless channelopathies. *Lancet Neurol.* **13**, 587–599 (2014).
22. D. L. Bennett, A. J. Clark, J. Huang, S. G. Waxman, S. D. Dib-Hajj, The role of voltage-gated sodium channels in pain signaling. *Physiol. Rev.* **99**, 1079–1151 (2019).
23. J. A. Black, N. Frézel, S. D. Dib-Hajj, S. G. Waxman, Expression of Nav1.7 in DRG neurons extends from peripheral terminals in the skin to central preterminal branches and terminals in the dorsal horn. *Mol. Pain* **8**, 82 (2012).
24. A. M. Rush, T. R. Cummins, S. G. Waxman, Multiple sodium channels and their roles in electrogenesis within dorsal root ganglion neurons. *J. Physiol.* **579**, 1–14 (2007).
25. A. J. Alexandrou, A. R. Brown, M. L. Chapman, M. Estacion, J. Turner, M. A. Mis, A. Wilbrey, E. C. Payne, A. Gutteridge, P. J. Cox, R. Doyle, D. Printzenhoff, Z. Lin, B. E. Marron, C. West, N. A. Swain, R. I. Storer, P. A. Stupple, N. A. Castle, J. A. Hounshell, M. Rivara, A. Randall, S. D. Dib-Hajj, D. Krafte, S. G. Waxman, M. K. Patel, R. P. Butt, E. B. Stevens, Subtype-selective small molecule inhibitors reveal a fundamental role for Nav1.7 in nociceptor electrogenesis, axonal conduction and presynaptic release. *PLOS ONE* **11**, e0152405 (2016).
26. J. Weiss, M. Pyrski, E. Jacobi, B. Bufe, V. Willnecker, B. Schick, P. Zizzari, S. J. Gossage, C. A. Greer, T. Leinders-Zufall, C. G. Woods, J. N. Wood, F. Zufall, Loss-of-function mutations in sodium channel $Na_v1.7$ cause anosmia. *Nature* **472**, –186, 190 (2011).
27. S. G. Waxman, Neuroscience: Channelopathies have many faces. *Nature* **472**, 173–174 (2011).
28. D. A. Eagles, C. Y. Chow, G. F. King, Fifteen years of Na_V 1.7 channels as an analgesic target: Why has excellent in vitro pharmacology not translated into in vivo analgesic efficacy? *Br. J. Pharmacol.* 1–20 (2020).
29. A. B. Vallbo, Microneurography: How it started and how it works. *J. Neurophysiol.* **120**, 1415–1427 (2018).
30. H. Bostock, K. Cikurel, D. Burke, Threshold tracking techniques in the study of human peripheral nerve. *Muscle Nerve.* **21**, 137–158 (1998).
31. J. D. Vardigan, A. K. Houghton, H. S. Lange, E. D. Adarayan, P. S. Pall, J. E. Ballard, D. A. Henze, J. M. Uslaner, Pharmacological validation of a novel nonhuman primate measure of thermal responsivity with utility for predicting analgesic effects. *J. Pain Res.* **11**, 735–741 (2018).
32. F. Zhao, M. A. Holahan, A. K. Houghton, R. Hargreaves, J. L. Evelhoch, C. T. Winkelmann, D. S. Williams, Functional imaging of olfaction by CBV fMRI in monkeys: Insight into the role of olfactory bulb in habituation. *Neuroimage* **106**, 364–372 (2015).
33. T. J. Greshock, J. Mulhearn, L. Guo, Z. Ting, D. Wang, R. M. Kim, M. E. Layton, M. J. Kelly, R. Anand, T. Jian, P. Nantermet, R. A. J. A. J. W. Won, G. Zhou, Diamino-alkylamino-linked arylsulfonamide compounds with selective activity in voltage-gated sodium channels, US 20180362518 A1 (2018).
34. C. J. Bungard, H. Y. Chen, J. M. Cox, L. Guo, M. J. Kelly, R. M. Kim, M. E. Layton, H. Liu, J. Liu, M. F. Patel, J. J. Perkins, D. Wang, W. Won, Y. Yu, T. Zhang, 4-Amino or 4-alkoxy-substituted aryl sulfonamide compounds with selective activity in voltage-gated sodium channels, US 2020117626 A1 (2020).
35. C. Chambers, I. Witton, C. Adams, L. Marrington, J. Kammonen, High-throughput screening of $Na_V1.7$ modulators using a giga-seal automated patch clamp instrument. *Assay Drug Dev. Technol.* **14**, 93–108 (2016).
36. J. Serra, M. Campero, J. Ochoa, H. Bostock, Activity-dependent slowing of conduction differentiates functional subtypes of C fibres innervating human skin. *J. Physiol.* **515**, 799–811 (1999).
37. M. D. Gee, B. Lynn, B. Cotsell, Activity-dependent slowing of conduction velocity provides a method for identifying different functional classes of C-fibre in the rat saphenous nerve. *Neuroscience* **73**, 667–675 (1996).
38. J. G. Thalhammer, S. A. Raymond, F. A. Popitz-bergez, G. R. Strichartz, Modality-dependent modulation of conduction by impulse activity in functionally characterized single cutaneous afferents in the rat. *Somatosens. Mot. Res.* **11**, 243–257 (1994).
39. C. Weidner, M. Schmelz, R. Schmidt, B. Hansson, H. O. Handwerker, H. E. Torebjörk, Functional attributes discriminating mechano-insensitive and mechano-responsive C nociceptors in human skin. *J. Neurosci.* **19**, 10184–10190 (1999).
40. B. Shim, M. Ringkamp, G. L. Lambrinos, T. V. Hartke, J. W. Griffin, R. A. Meyer, Activity-dependent slowing of conduction velocity in uninjured L4 C fibers increases after an L5 spinal nerve injury in the rat. *Pain* **128**, 40–51 (2007).
41. L. Cao, A. McDonnell, A. Nitzsche, A. Alexandrou, P. P. Saintot, A. J. C. Loucif, A. R. Brown, G. Young, M. Mis, A. Randall, S. G. Waxman, P. Stanley, S. Kirby, S. Tarabar, A. Gutteridge, R. Butt, R. M. McKernan, P. Whiting, Z. Ali, J. Bilsland, E. B. Stevens, Pharmacological reversal of a pain phenotype in iPSC-derived sensory neurons and patients with inherited erythromelalgia. *Sci. Transl. Med.* **8**, 335ra356 (2016).
42. M. Campero, J. Serra, H. Bostock, J. L. Ochoa, Partial reversal of conduction slowing during repetitive stimulation of single sympathetic efferents in human skin. *Acta Physiol. Scand.* **182**, 305–311 (2004).
43. D. A. Yablonskiy, E. M. Haacke, Theory of NMR signal behavior in magnetically inhomogeneous tissues: The static dephasing regime. *Magn. Reson. Med.* **32**, 749–763 (1994).
44. N. A. Swain, D. Batchelor, S. Beaudoin, B. M. Bechle, P. A. Bradley, A. D. Brown, B. Brown, K. J. Butcher, R. P. Butt, M. L. Chapman, S. Denton, D. Ellis, S. R. G. Galan, S. M. Gaulier, B. S. Greener, M. J. de Groot, M. S. Glossop, I. K. Gurrell, J. Hannam, M. S. Johnson, Z. Lin, C. J. Markworth, B. E. Marron, D. S. Millan, S. Nakagawa, A. Pike, D. Printzenhoff, D. J. Rawson, S. J. Ransley, S. M. Reister, K. Sasaki, R. I. Storer, P. A. Stupple, C. W. West, Discovery of clinical candidate 4-[2-(5-amino-1*H*-pyrazol-4-yl)-4-chlorophenoxy]-5-chloro-2-fluoro-*N*-1,3-thiazol-4 -ylbenzenesulfonamide (PF-05089771): Design and optimization of diaryl ether aryl sulfonamides as selective inhibitors of $Na_V1.7$. *J. Med. Chem.* **60**, 7029–7042 (2017).
45. A. McDonnell, S. Collins, Z. Ali, L. Iavarone, R. Surujbally, S. Kirby, R. P. Butt, Efficacy of the $Na_v1.7$ blocker PF-05089771 in a randomised, placebo-controlled, double-blind clinical study in subjects with painful diabetic peripheral neuropathy. *Pain* **159**, 1465–1476 (2018).
46. K. McCormack, S. Santos, M. L. Chapman, D. S. Krafte, B. E. Marron, C. W. West, M. J. Krambis, B. M. Antonio, S. G. Zellmer, D. Printzenhoff, K. M. Padilla, Z. Lin, P. K. Wagoner, N. A. Swain, P. A. Stupple, M. de Groot, R. P. Butt, N. A. Castle, Voltage sensor interaction site for selective small molecule inhibitors of voltage-gated sodium channels. *Proc. Natl. Acad. Sci. U.S.A.* **110**, E2724–E2732 (2013).

47. P. Siebenga, G. van Amerongen, J. L. Hay, A. McDonnell, D. Gorman, R. Butt, G. J. Groeneveld, Lack of detection of the analgesic properties of PF-05089771, a selective $Na_v1.7$ inhibitor, using a battery of pain models in healthy subjects. *Clin. Transl. Sci.* **13**, 318–324 (2020).
48. H. M. Jones, R. P. Butt, R. W. Webster, I. Gurrell, P. Dzygiel, N. Flanagan, D. Fraier, T. Hay, L. E. Iavarone, J. Luckwell, H. Pearce, A. Phipps, J. Segelbacher, B. Speed, K. Beaumont, Clinical micro-dose studies to explore the human pharmacokinetics of four selective inhibitors of human Nav1.7 voltage-dependent sodium channels. *Clin. Pharmacokinet.* **55**, 875–887 (2016).
49. S. Ahuja, S. Mukund, L. Deng, K. Khakh, E. Chang, H. Ho, S. Shriver, C. Young, S. Lin, J. P. Johnson Jr., P. Wu, J. Li, M. Coons, C. Tam, B. Brillantes, H. Sampang, K. Mortara, K. K. Bowman, K. R. Clark, A. Estevez, Z. Xie, H. Verschoof, M. Grimwood, C. Dehnhardt, J.-C. Andrez, T. Focken, D. P. Sutherlin, B. S. Safina, M. A. Starovasnik, D. F. Ortwine, Y. Franke, C. J. Cohen, D. H. Hackos, C. M. Koth, J. Payandeh, Structural basis of Nav1.7 inhibition by an isoform-selective small-molecule antagonist. *Science* **350**, aac5464 (2015).
50. E. Garcia-Perez, P. S. Pall, R. Sola, M. Sumalla, A. Houghton, J. Serra, A microneurography inter-species study comparing the relative distribution of C-nociceptor types and parameters of activitydependent slowing (ADS) of conduction velocity reflecting different axonal membrane properties in mice, rat, non-human primate and healthy subjects, paper presented at the Society for Neuroscience Annual Meeting 2017, Washington, DC, Poster 397.09.
51. A. J. Roecker, M. E. Layton, M. J. Kelly, J. E. Pero, T. Zhang, R. L. Kraus, Y. Li, R. Klein, M. K. Clements, C. D. Daley, J. Wang, E. Finger, J. M. Majercak, V. Santarelli, I. Gregan, M. Cato, T. Filzen, A. Jovanovska, J. Ballard, D. Wang, F. Zhao, L. A. Joyce, E. C. Sherer, X. Peng, X. Wang, A. K. Houghton, C. S. Burgey, Discovery of Novel Arylsulfonamide Nav1.7 Inhibitors: In Vitro-In Vivo Correlations, Development of Multiparameter Optimization (MPO) Methods, and Optimization of Selectivity Profile, in *256th ACS National Meeting and Exposition, Boston, MA, August 20, 2018 (oral presentation* (2018).
52. W.-H. Xiao, G. J. Bennett, Persistent low-frequency spontaneous discharge in A-fiber and C-fiber primary afferent neurons during an inflammatory pain condition. *Anesthesiology* **107**, 813–821 (2007).
53. R. H. LaMotte, J. N. Campbell, Comparison of responses of warm and nociceptive C-fiber afferents in monkey with human judgments of thermal pain. *J. Neurophysiol.* **41**, 509–528 (1978).
54. H. S. Ahn, J. A. Black, P. Zhao, L. Tyrrell, S. G. Waxman, S. D. Dib-Hajj, Nav1.7 is the predominant sodium channel in rodent olfactory sensory neurons. *Mol. Pain* **7**, 32 (2011).
55. J. Gingras, S. Smith, D. J. Matson, D. Johnson, K. Nye, L. Couture, E. Feric, R. Yin, B. D. Moyer, M. L. Peterson, J. B. Rottman, R. J. Beiler, A. B. Malmberg, S. I. McDonough, Global Nav1.7 knockout mice recapitulate the phenotype of human congenital indifference to pain. *PLOS ONE* **9**, e105895 (2014).
56. Y. P. Goldberg, J. MacFarlane, M. L. MacDonald, J. Thompson, M.-P. Dube, M. Mattice, R. Fraser, C. Young, S. Hossain, T. Pape, B. Payne, C. Radomski, G. Donaldson, E. Ives, J. Cox, H. B. Younghusband, R. Green, A. Duff, E. Boltshauser, G. A. Grinspan, J. H. Dimon, B. G. Sibley, G. Andria, E. Toscano, J. Kerdraon, D. Bowsher, S. N. Pimstone, M. E. Samuels, R. Sherrington, M. R. Hayden, Loss-of-function mutations in the Nav1.7 gene underlie congenital indifference to pain in multiple human populations. *Clin. Genet.* **71**, 311–319 (2007).
57. J. Serra, M. Campero, H. Bostock, J. Ochoa, Two types of C nociceptors in human skin and their behavior in areas of capsaicin-induced secondary hyperalgesia. *J. Neurophysiol.* **91**, 2770–2781 (2004).
58. T. Hummel, G. Kobal, H. Gudziol, A. Mackay-Sim, Normative data for the "Sniffin' Sticks" including tests of odor identification, odor discrimination, and olfactory thresholds: An upgrade based on a group of more than 3,000 subjects. *Eur. Arch. Otorhinolaryngol.* **264**, 237–243 (2007).
59. F. Zhao, M. A. Holahan, X. Wang, J. M. Uslaner, A. K. Houghton, J. L. Evelhoch, C. T. Winkelmann, C. D. G. Hines, fMRI study of the role of glutamate NMDA receptor in the olfactory processing in monkeys. *PLOS ONE* **13**, e0198395 (2018).
60. R. L. Wasserstein, A. L. Schirm, N. A. Lazar, Moving to a world beyond "$p < 0.05$". *Am. Stat.* **73**, 1–19 (2019).
61. J. Serra, H. Bostock, X. Navarro, Microneurography in rats: A minimally invasive method to record single C-fiber action potentials from peripheral nerves in vivo. *Neurosci. Lett.* **470**, 168–174 (2010).

Acknowledgments: We would like to thank H. Lange for compound preparation and data analysis for rhesus thermode experiments, D. Holder and K. Chen for microneurography statistical analyses, S. Donavan for expert tissue culture, and C. T. John for compound formulation. We thank the MRL, WP veterinarian associates S. Jendrowski, T. Montgomery, W. Watson, and L. Carangia for help with instrumenting and monitoring the microneurography animals and for assistance with dosing and blood draws. K. Lodge provided NHP nerve exposure training to the biologists. **Funding:** R.L.K., F.Z., P.S.P., D.Z., J.D.V., A.D., Y.L., C.D., J.E.B., M.K.C., R.M.K., M.A.H., T.J.G., R.M.K., M.E.L., C.S.B., D.A.H., and A.K.H are employed by Merck Sharp & Dohme Corp., a subsidiary of Merck & Co. Inc., Kenilworth, NJ, USA. **Author contributions:** R.L.K., Y.L., and C.D. designed and executed Qube experiments and performed data analysis. M.K.C. and R.M.K. designed and executed manual patch clamp experiments and performed data analysis. P.S.P., J.S., D.A.H., A.K.H., J.E.B., and D.Z. designed and executed rhesus microneurography experiments and performed data analysis. J.D.V., P.S.P., D.A.H., A.K.H., and J.E.B. designed and executed rhesus thermal responsivity experiments and performed data analysis. D.A.H., A.K.H., and A.D. designed and executed TT experiments and performed data analysis. F.Z., M.A.H., D.A.H., A.K.H., and J.E.B. designed, executed, and analyzed rhesus fMRI studies. T.J.G., R.M.K., M.E.L., and C.S.B. designed and synthesized SSCI-1 and SSCI-2. R.L.K., F.Z., P.S.P., J.D.V., C.D., M.K.C., R.K., C.S.B., J.E.B., J.S., D.A.H., and A.K.H. wrote the manuscript. **Competing interests:** R.L.K, F.Z., P.S.P., D.Z., J.D.V., A.D., Y.L., C.D., J.E.B., M.K.C., R.M.K., M.A.H., T.J.G., R.M.K., M.E.L., C.S.B., D.A.H., and A.K.H. are employed by Merck Sharp & Dohme Corp., a subsidiary of Merck & Co. Inc., Kenilworth, NJ, USA. J.S. was paid as a consultant to establish microneurography in nonhuman primates at Merck Sharp & Dohme Corp., a subsidiary of Merck & Co. Inc., Kenilworth, NJ, USA. Patents US 20180362518 A1, Diamino-Alkylamino-Linked Arylsulfonamide Compounds with Selective Activity in Voltage-Gated Sodium Channels (*33*), and US 2020117626 A1, 4-Amino or 4-Alkoxy-Substituted Aryl Sulfonamide Compounds with Selective Activity in Voltage-Gated Sodium Channels (*34*), are related to this work. **Data and materials availability:** All data associated with this study are present in the paper or the Supplementary Materials.

Submitted 29 May 2019
Resubmitted 3 June 2020
Accepted 20 February 2021
Published 19 May 2021
10.1126/scitranslmed.aay1050

Citation: R. L. Kraus, F. Zhao, P. S. Pall, D. Zhou, J. D. Vardigan, A. Danziger, Y. Li, C. Daley, J. E. Ballard, M. K. Clements, R. M. Klein, M. A. Holahan, T. J. Greshock, R. M. Kim, M. E. Layton, C. S. Burgey, J. Serra, D. A. Henze, A. K. Houghton, $Na_v1.7$ target modulation and efficacy can be measured in nonhuman primate assays. *Sci. Transl. Med.* **13**, eaay1050 (2021).

Science Translational Medicine

$Na_V1.7$ target modulation and efficacy can be measured in nonhuman primate assays

Richard L. Kraus, Fuqiang Zhao, Parul S. Pall, Dan Zhou, Joshua D. Vardigan, Andrew Danziger, Yuxing Li, Christopher Daley, Jeanine E. Ballard, Michelle K. Clements, Rebecca M. Klein, Marie A. Holahan, Thomas J. Greshock, Ronald M. Kim, Mark E. Layton, Christopher S. Burgey, Jordi Serra, Darrell A. Henze and Andrea K. Houghton

Sci Transl Med **13**, eaay1050.
DOI: 10.1126/scitranslmed.aay1050

Improving target engagement

Successful target engagement in vivo is a critical step in drug development. Targeting the voltage-gated sodium channel 1.7 ($Na_V1.7$) with specific inhibitors holds promises for the treatment of chronic pain. However, inhibitors with good in vitro properties failed in the clinic. Now, Kraus *et al.* developed a protocol to guide dose calculation and determine target engagement of $Na_V1.7$ inhibitors in nonhuman primates that could be translated to the clinic. The authors used microneurography of C-fibers, heat responsivity, and fMRI of the olfactory bulb to determine the plasma concentration required to produce channel inhibition of two potent $Na_V1.7$ inhibitors. Adapted to humans, the results will help the development and interpretation of clinical trials testing $Na_V1.7$ inhibitors.

Science Translational Medicine (ISSN 1946-6242) is published by the American Association for the Advancement of Science, 1200 New York Avenue NW, Washington, DC 20005. The title *Science Translational Medicine* is a registered trademark of AAAS.